



## Data in Brief

# Transcriptional profiling of MEF2-regulated genes in human neural progenitor cells derived from embryonic stem cells



Shing Fai Chan <sup>a,1</sup>, Xiayu Huang <sup>b,1</sup>, Scott R. McKercher <sup>a</sup>, Rameez Zaidi <sup>a</sup>, Shu-ichi Okamoto <sup>a</sup>, Nobuki Nakanishi <sup>a</sup>, Stuart A. Lipton <sup>a,\*</sup>

<sup>a</sup> Neuroscience and Aging Research Center, Sanford-Burnham Medical Research Institute, 10901 North Torrey Pines Road, La Jolla, CA 92037, USA

<sup>b</sup> Bioinformatics and Systems Biology Program, Sanford-Burnham Medical Research Institute, 10901 North Torrey Pines Road, La Jolla, CA 92037, USA

## ARTICLE INFO

## Article history:

Received 24 October 2014

Accepted 30 October 2014

Available online 7 November 2014

## Keywords:

MEF2

Transcription factor

Microarray

Gene expression

Human neural stem cells

Neuronal differentiation

## ABSTRACT

The myocyte enhancer factor 2 (MEF2) family of transcription factors is highly expressed in the brain and constitutes a key determinant of neuronal survival, differentiation, and synaptic plasticity. However, genome-wide transcriptional profiling of MEF2-regulated genes has not yet been fully elucidated, particularly at the neural stem cell stage. Here we report the results of microarray analysis comparing mRNAs isolated from human neural progenitor/stem cells (hNPCs) derived from embryonic stem cells expressing a control vector versus progenitors expressing a constitutively-active form of MEF2 (MEF2CA), which increases MEF2 activity. Microarray experiments were performed using the Illumina Human HT-12 V4.0 expression beadchip (GEO#: GSE57184). By comparing vector-control cells to MEF2CA cells, microarray analysis identified 1880 unique genes that were differentially expressed. Among these genes, 1121 genes were up-regulated and 759 genes were down-regulated. Our results provide a valuable resource for identifying transcriptional targets of MEF2 in hNPCs.

© 2014 The Authors. Published by Elsevier Inc. This is an open access article under the CC BY-NC-ND license (<http://creativecommons.org/licenses/by-nc-nd/3.0/>).

Specifications	
Organism/cell line/tissue	Homo sapiens/ human neural progenitor cells derived from embryonic stem cells (hNPCs)
Sex	N/A
Sequencer or array type	Microarray: Illumina HumanHT-12 V4.0 expression beadchip
Data format	Raw and processed
Experimental factors	hNPCs expressing control vector versus constitutively-active MEF2 (MEF2CA)
Experimental features	We performed a microarray analysis to identify genes differentially expressed in hNPCs expressing MEF2CA versus control vector
Consent	N/A
Sample source location	La Jolla, CA, USA

## Experimental design, materials and methods

### *Culture and transfection of human neural progenitor cells (hNPCs) derived from embryonic stem cells*

We cultured H9 human embryonic stem cells (WiCell Research Institute) and then induced neural differentiation into neural progenitor cells (hNPCs), as previously described [1]. We transfected the hNPCs with control vector- or constitutively active MEF2 (MEF2CA)-tdTomato mammalian expression constructs by electroporation using the human stem cell Nucleofector® kit, according to the manufacturer's instructions (Lonza/Amama Biosystem). On the third day after transfection, the cells were incubated with Annexin V-FITC, according to manufacturer's instructions (BD Pharmingen). Next, tdTomato-positive cells and Annexin V-FITC-negative cells were sorted and selected on a FACS Advantage SE DiVa (BD Biosciences) with a 100 µm nozzle at 13 psi.

tdTomato and Annexin V-FITC were excited at 488 nm and detected with standard PE and FITC emission filters, respectively.

### *RNA extraction, purification, and quality verification*

We extracted total RNA from transfected hNPCs using Trizol Reagent and the PureLink™ RNA Mini Kit, according to the manufacturer's

## Direct link to deposited data

Deposited data can be found in the Gene Expression Omnibus (GEO) database: <http://www.ncbi.nlm.nih.gov/geo/query/acc.cgi?acc=GSE57184>

\* Corresponding author. Tel.: +1 858 795 5261.

E-mail address: [slipton@sanfordburnham.org](mailto:slipton@sanfordburnham.org) (S.A. Lipton).

<sup>1</sup> These authors contributed equally to this work.

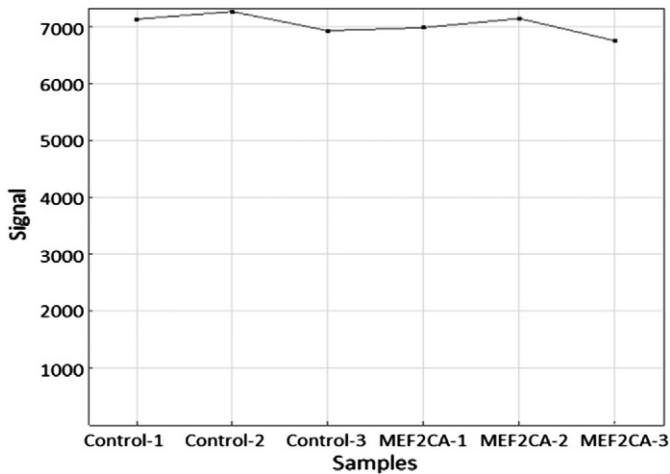


**Fig. 1.** GenomeStudio control summary plot. Signal intensity values (y-axis) of hybridization controls are consistently high across all six samples of control-1, -2, -3 and MEF2CA-1, -2, -3 (x-axis).

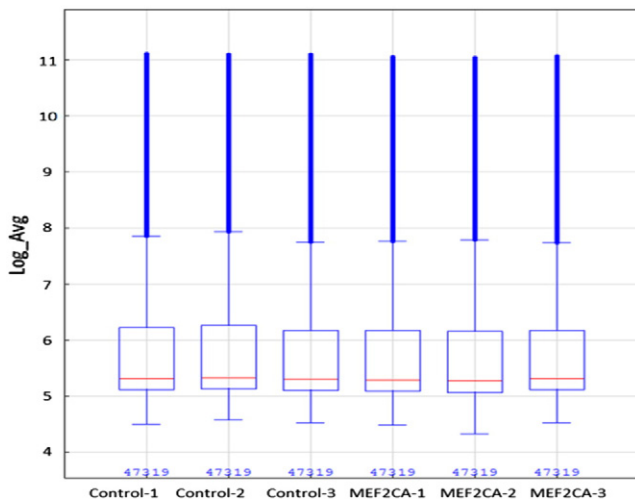


**Fig. 2.** Logarithmic box plot of mean signal across all samples. Mean signal intensity of all assays is plotted for each of six samples (control-1, -2, -3 and MEF2CA-1, -2, -3) (x-axis). A complete view of median values, percentile and the outlier points (thick vertical blue lines) of all samples is illustrated with a log Avg signal plot.

instructions (Invitrogen). After checking RNA concentration and purity on a NanoDrop 2000c (Thermo Fisher Scientific), RNA quality and quantity were further validated using an Experion Automated Electrophoresis Station and Experion RNA Analysis Kits (BioRAD Laboratories).

#### mRNA profiling by microarray analysis and data processing

We prepared labeled cRNA from 500 ng of RNA using the Illumina® RNA amplification kit (Ambion/ Life Technologies). We then hybridized the labeled cRNA (750 ng) overnight, at 58 °C, to HumanHT-12 Expression BeadChips (>46,000 gene transcripts; Illumina), following the manufacturer's instructions. We subsequently washed and developed BeadChips with fluorolink streptavidin-Cy3 (GE Healthcare) and used an Illumina BeadArray Reader to scan the BeadChips. We then collected and analyzed the microarray data as follows: we used the software tool GenomeStudio V2011.1 (Illumina) for gene expression quantification and its in-built plotting features for data quality control (QC), including Control Summary Plot (Fig. 1) and Box Plot (Fig. 2). We found that all 6 samples (control-1, -2, -3 and MEF2CA-1, -2, -3) were of good quality according to GenomeStudio QC guidelines [2]. The sample probe text file generated from GenomeStudio was processed using Genespring GX 11.5 (Agilent Technologies) and probes with detection  $p$ -values  $\leq 0.05$  were used for further statistical analysis. Log<sub>2</sub> transformation was applied to probe level intensities of all 6 samples in order to generate identical distributions for comparison, which was then followed by quantile normalization [3]. Statistical significance of the differential expression of genes between control and MEF2CA samples was determined by Student's unpaired  $t$  test. The  $p$ -values were corrected via application of the Benjamini and Hochberg false discovery rate (FDR) algorithm [4]. The extent and direction of differential expression between the groups were determined by calculating a fold change value (Fig. 3). A fold change of  $\geq 1.5$  and an FDR-adjusted  $p$ -value of  $\leq 0.05$  were used as criteria to indicate differential expression between the two groups. We list the identified 1121 up-regulated and 759 down-regulated differentially expressed genes in Table 1.

#### Discussion

Here we describe the genome-wide transcriptional profiling of MEF2-regulated genes in hNPCs derived from human embryonic stem cells. This data set is the first microarray analysis to identify target genes that are differentially expressed and regulated by MEF2 in hNPCs. MEF2 transcription factors are known to be neurogenic and anti-apoptotic; thus, their transcriptional targets in neural

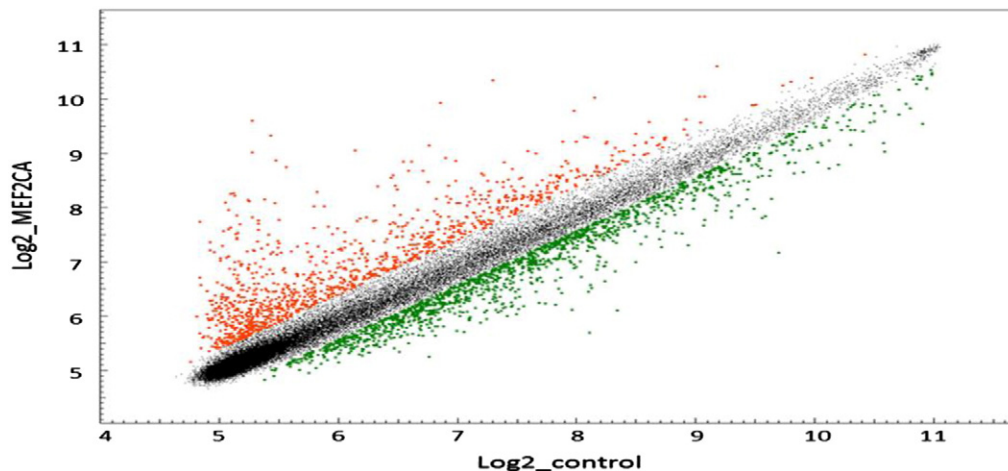


**Fig. 3.** Scatter plot of relative gene expression between control and MEF2CA samples. The red dots and green dots represent 1.5 fold up-regulated and down-regulated genes (adjusted  $p \leq 0.05$ ), respectively.



Table 1 (continued)

List of differentially expressed genes (adjusted $p \leq 0.05$ ) with fold change $\geq 1.5$ identified from microarray analysis	
1121 up-regulated genes	759 down-regulated genes
RAB3GAP1, RAB4A, RAD23B, RALGAP1, RAP2A, RAPGEF2, RARB, RASA2, RASGRP2, RASGRP3, RASL12, RBM20, RBM46, RBM9, RBMS3, RDH12, RDH5, REEP1, RELN, RERG, RERGL, REV1, RFPL15, RFTN1, RFTN2, RGS20, RHCE, RHEB, RHOBTB1, RHOBTB3, RHOQ, RHPN2, RICH2, RIOK1, RIOK3, RN559, RN7SK, RNASEN, RNF103, RNF11, RNF115, RNF141, RNF17, RNP3C, RPA4, RPS29, Rragd, Rras2, Rsrc1, RTN2, RTN4, RTTN, RUNC3B, RYR1, S100A10, SAMD4A, SBK1, SCAMP1, SCARNA11, SCARNA13, SCARNA14, SCARNA21, SCARNA8, SCHIP1, SDC2, SDCBP, SDHC, SECISBP2L, SEH1L, SEMA4D, SEMA5A, SEMAGC, SEPP1, SEPSECS, SEPT4, SEPT5, SEPT7, SEPW1, SERPINB7, SERPINH1, SERTAD2, SETBP1, SFRS2IP, SFTA2, SGGC, SH2D3C, SH3RF3, SHISA2, SHRM, SHROOM3, SIPA1L2, SLC12A2, SLC16A3, SLC16A7, SLC17A2, SLC20A2, SLC22A11, SLC22A2, SLC23A2, SLC25A14, SLC25A34, SLC25A4, SLC26A3, SLC26A6, SLC29A1, SLC2A11, SLC2A12, SLC35F5, SLC40A1, SLC41A1, SLC7A8, SLC9A9, SLIT2, SLITRK5, SLMO1, SLU7, SMCHD1, SMEK2, SMG1, SMOC1, SMYD1, SNAP25, SNAPC1, SNORA12, SNORA79, SNORD3A, SNORD3C, SNORD3D, SNTB2, SNTG1, SNX25, SNX27, SOCS2, SOD3, SORBS2, SORT1, SOS1, SOSTDC1, SPAG16, SPAG6, SPATA17, SPATA5, SPATA9, SPC25, SPHAR, SPIB, SPINT2, SPOCK1, SPPL2A, SRFBP1, SRRM4, SSSFA2, ST3GAL6, ST6GAL1, ST7, STARD7, STIM1, STK3, STK38, STK38L, STOM, SUMF1, SUMO3, SUPT3H, SUSD1, SYNC1, SYNEM, SYNPO2, SYNPO2L, SYPL2, SYT1, SYT17, SYT4, SYTL2, SYTL4, TACC2, TACSTD2, TAF1B, TAF7L, TAGLN, TAP1, TBC1D15, TBXAS1, TCAP, TDRD5, TDRD9, TESK2, TG, THADA, TIAF1, TIAM2, TIGD4, TJP2, TMC6, TMC7, TMEM117, TMEM119, TMEM144, TMEM173, TMEM2, TMEM30B, TMEM35, TMEM38B, TMEM47, TMOD1, TMPRSS11A, TMTC1, TNFAIP6, TNFRSF11B, TNMD, TNNC1, TNIN3K, TOB1, TOP2B, TOR1AIP2, TOX3, TPD52L1, TRAK1, TRAPP9C, TRIM29, TRIM33, TRPC1, TRPC6, TRPM4, TSC22D2, TSGA10, TSPAN13, TSPAN3, TSPAN7, TUBB6, TUSC3, TWSG1, TXNDC11, TXNDC12, TXNDC16, TYRP1, UACA, UBA6, UBE2E1, UBE2H, UBE2J1, UBR3, ULK4, USP13, USP6NL, UTP11L, VBP1, VCL, VCX, VCX2, VCX3A, VCX-C, VCY, VEZT, VGLL2, VNN2, VOPP1, VPS26B, VTCN1, WDFY3, WDR17, WDR37, WDR62, WEE2, WFDC1, WFS1, WIPF3, WNT5B, WWC1, XIRP1, XKR6, YIPF7, YPEL5, ZAK, ZBTB20, ZC3H12C, ZCCHC11, ZDHHC17, ZFPC3H1, ZFP36, ZNF280C, ZNF30, ZNF330, ZNF364, ZNF385B, ZNF533, ZNF650, ZNF81, ZNRF2, ZRANB1, ZSWIM6	PTGIS, PTGS2, PTHLH, PTPRE, PTPRU, PTTG1, PTTG3P, RAB22A, RAB27A, RAB7B, RAD51AP1, RAD54L, RANGAP1, RARRRES2, RARRRES3, RASL10A, RBBP4, RBBP8, RDH10, RELB, REM1, RGM, RGS17, RGS4, RHOJ, RHOU, RIPK2, ROR2, RPL22L1, RPL36A, RRM1, RRM2, RSAD2, RSPO3, RUNX2, S100A13, S1PR3, SAMD9, SAMD9L, SCARA3, SCG5, SCN9A, SCXA, SDC1, SEC14L2, SEL1L3, SELM, SEMA3C, SEMA7A, SEPT3, SERPINA3, SERPING1, SERTAD4, SFRP1, SFRP2, SGK, SGK1, SGPP2, SH3PXD2B, SHANK3, SHMT2, SIK1, SLAMF8, SLC12A8, SLC15A3, SLC16A9, SLC1A3, SLC20A1, SLC22A17, SLC22A4, SLC25A24, SLC2A5, SLC31A2, SLC35F2, SLC39A14, SLC43A3, SLC5A6, SLC6A9, SLC7A5, SLC7A7, SNAI2, SOD2, SOX3, SOX9, SP100, SP110, SPANX, SPARC, SPIN4, SPON1, SPP1, SPSB1, SRGN, SRPX2, SSBP4, SSX2IP, STAT1, STAT2, STC1, STEAP1, STEAP2, STIL, STOX2, STRA6, STXBP6, SULF1, SULF2, SYT7, TAC1, TAC3, TACC3, TAP1, TAP2, TAPBP, TCEAL7, TCF21, TDO2, TFF3, TFPF2, TGF3B, TGFBR2, TGM2, THBS4, TIMP3, TJAP1, TK1, TMEM154, TMEM158, TMEM163, TMEM16A, TMEM217, TMEM4, TMEM90B, TNC, TNFAIP3, TNFRSF10B, TNFRSF19, TNFRSF8, TNFSF10, TNFSF11, TNFSF13B, TNFSF9, TNIP3, TNPO1, TOP2A, TPR, TPX2, TRAM2, TREM1, TRIB3, TRIM15, TRIM22, TRIM5, TRIM9, TRIP13, TROAP, TSHZ2, TSHZ3, TSKU, TSPAN6, TXNIP, TYMS, UAP1, UBA7, UBASH3B, UBE2C, UBE2L6, UBE2T, UPP1, USP1, USP18, VANGL2, VARS, VASH1, VAT1L, VCAM1, VCAN, VEGFA, VGF, VRK1, WARS, WEE1, WNT5A, XAF1, XRCC3, ZMIZ1, ZNF365, ZNF697, ZP4, ZSWIM4, ZWILCH

progenitors that mediate these effects are of great biological interest. Accordingly, our results reveal that MEF2 target genes are enriched in pathways involved in nervous system development and function [5]. Recently, dominant mutations in *MEF2C* (5q14.3 microdeletions) resulting in haploinsufficiency have been linked to autism spectrum disorder (ASD) in multiple human cases [6–8]. Additionally, transcriptome analyses of human ASD brains have identified *MEF2C* as a “node” connecting various genes affected in autism [9,10]. Therefore, the profiling of transcriptional targets of MEF2 at the neural stem cell stage, as studied here, may reveal potential therapeutic targets for ASD.

### Conflict of interest

The authors declare no conflicts of interest.

### Acknowledgments

This work was supported in part by a grant from the California Institute for Regenerative Medicine (grant no. TR4-06788), the National Institutes of Health (grant no. R01 NS086890), and a Brain and Behavior Research Foundation NARSAD Distinguished Investigator Award (BBRF 2014 to S.A.L.), a Shiley–Marcos Alzheimer’s Disease Research Center (UCSD) Pilot Award, and a National Institutes of Health grant R21 MH102672 (to S.-i.O.). We thank Anthony Nutter (Sanford-Burnham) for helpful discussions and proofreading of the manuscript.

### References

- [1] E.G. Cho, J.D. Zaremba, S.R. McKercher, M. Talantova, S. Tu, E. Masliah, S.F. Chan, N. Nakanishi, A. Tersikh, S.A. Lipton, *MEF2C* enhances dopaminergic neuron

- differentiation of human embryonic stem cells in a parkinsonian rat model. *PLoS One* 6 (2011) e24027.
- [2] Gene expression microarray data quality control. [http://res.illumina.com/documents/products/technotes/technote\\_gene\\_expression\\_data\\_quality\\_control.pdf](http://res.illumina.com/documents/products/technotes/technote_gene_expression_data_quality_control.pdf).
- [3] B.M. Bolstad, R.A. Irizarry, M. Astrand, T.P. Speed, A comparison of normalization methods for high density oligonucleotide array data based on variance and bias. *Bioinformatics* 19 (2003) 185–193.
- [4] Y. Benjamini, Y. Hochberg, Controlling the false discovery rate: a practical and powerful approach to multiple testing. *J. R. Statist. Soc. B* 57 (1995) 289–300.
- [5] S. Okamoto, T. Nakamura, P. Cieplak, S.F. Chan, E. Kalashnikova, L. Liao, S. Saleem, X. Han, A. Clemente, A. Nutter, S. Sances, C. Brechtel, D. Haus, F. Haun, S. Sanz-Blasco, X. Huang, H. Li, J.D. Zaremba, J. Cui, Z. Gu, R. Nikzad, A. Harrop, S.R. McKercher, A. Godzik, J.R. Yates III, S.A. Lipton, S-Nitrosylation-mediated redox transcriptional switch modulates neurogenesis and neuronal cell death. *Cell Rep.* 8 (2014) 217–228.
- [6] N. Le Meur, M. Holder-Espinasse, S. Jaillard, A. Goldenberg, S. Joriot, P. Amati-Bonneau, A. Guichet, M. Barth, A. Charollais, H. Journel, S. Auvin, C. Boucher, J.P. Kerckaert, V. David, S. Manouvrier-Hanu, P. Saugier-Verber, T. Frébourg, C. Dubourg, J. Andrieux, D. Bonneau, *MEF2C* haploinsufficiency caused by either microdeletion of the 5q14.3 region or maturation is responsible for severe mental retardation with stereotypic movements, epilepsy, and/or cerebral malformations. *J. Med. Genet.* 47 (2010) 22–29.
- [7] B.A. Nowakowska, E. Obersztyjn, K. Szymańska, M. Bekiesińska-Figatowska, Z. Xia, C.B. Ricks, E. Bocian, D.W. Stockton, K. Szczałuba, M. Nawara, A. Patel, D.A. Scott, S.W. Cheung, T.P. Bohan, P. Stankiewicz, Severe mental retardation, seizures, and hypotonia due to deletions of *MEF2C*. *Am. J. Med. Genet. B Neuropsychiatr. Genet.* 153B (2010) 1042–1051.
- [8] M. Zweier, A. Gregor, C. Zweier, H. Engels, H. Sticht, E. Wohlleber, E.K. Bijlsma, S.E. Holder, M. Zenker, E. Rossier, U. Grashoff, D.S. Johnson, L. Robertson, H.V. Firth, Cornelia Kraus, A.B. Ekici, A. Reis, A. Rauch, Mutations in *MEF2C* from the 5q14.3q15 microdeletion syndrome region are a frequent cause of severe mental retardation and diminish *MECP2* and *CDKL5* expression. *Hum. Mutat.* 31 (2010) 722–733.
- [9] I. Voineagu, X. Wang, P. Johnston, J.K. Lowe, Y. Tian, S. Horvath, J. Mill, R.M. Cantor, B.J. Blencowe, D.H. Geschwind, Transcriptomic analysis of autistic brain reveals convergent molecular pathology. *Nature* 474 (2011) 380–384.
- [10] N.N. Parikshak, R. Luo, A. Zhang, H. Won, J.K. Lowe, V. Chandran, S. Horvath, D.H. Geschwind, Integrative functional genomic analyses implicate specific molecular pathways and circuits in autism. *Cell* 155 (2013) 1008–1021.